jet INTL JOURNAL OF ELECTRONICS AND TELECOMMUNICATIONS, 2024, VOL. 70, NO. 4, PP. 987–995
Manuscript received July 16, 2024; revised October 2024. doi: 10.24425/ijet.2024.152086

Advanced design and analysis of dual element MIMO antenna for Ultra-Wideband Applications

Ramamohan B, and Siva Ganga Prasad M

***Abstract*—This investigation uses the Genetic Optimization Method to convert a wide-band MIMO antenna into a UWB (3.1GHz–10.6 GHz) MIMO antenna. Initially, a 22 × 42, mm^2 wideband 2X2 MIMO antenna was designed using commercial Flame Retardant-4 material. The structure of the antenna patch was designed using half-circular forms on the half-ground plane. The designed MIMO antenna operates throughout a large frequency range of 4.8-9.8 GHz. While it was successful in achieving broad band characteristics, this MIMO antenna was unable to reach ultra-wide band characteristics. The MIMO antenna was operated in UWB ranges by a parametric study, which indicated that the resonating characteristics can be significantly modified by inserting a rectangular slot into the ground plane. Throughout the operational range, it was important to be concerned about improved gain and good isolation. Accordingly, optimization was carried out in order to accomplish the essential, multi-objective goals. The difficult multi-objective design goal is now reduced to an optimization challenge by means of genetic algorithm based random search. One of the performance goals that this optimization strategy aimed to fulfil was an increase in isolation to -20 dB across the entire Ultra-Wideband, with S11 being below -10 dB from 3.1 to 10.6 GHz. It is recommended to randomly select the parameters from their respective ranges for this work. This led to the selection of an optimizer based on random searches. In the operating range, the UWB has a respectable gain of 4 dB to 6 dB and increased isolation to -20 dB, according to the genetic algorithm optimizer's execution of the predefined multiple-objective task.**

***Keywords*—MIMO antenna; Optimization; Mutual coupling; Ultra-Wideband; Isolation**

I. Introduction

WHEN compared to more standard wireless methods, ultra-wideband (UWB) technology offers greater communication throughput while using significantly less power. Its use of a broad-spectrum, ultra-short pulse with very little energy means it causes less interference with other technologies that rely on short-range wireless communication, like wireless personal area networks and location tracking. The commercial radar industry was the first to embrace ultra-wideband technology, which found its way into consumer electronics and wireless personal area networks. As time has progressed, it has found new uses in fields as diverse as radar systems, wireless communication, and even medical equipment. Ultra-Wideband had a monopoly on military use until 2001, when it began to see widespread use across industries because of technological advancements. The Federal Communications Commission (FCC) opened the door to the public's commercial usage of ultra-wideband technology in 2002. The U.S. uses ultra-wideband spectrum, which is defined by the FCC and ranges from less than 3.1 GHz to 10.6 GHz [1] [2]. Numerous applications were granted access to this spectrum, including Wireless Personal Area Networks (WPANs), location tracking, and high-speed data transport.When used in a vehicle, the UWB MIMO antenna can manage both high-speed data and multimedia communications. The UWB MIMO antenna may work well for car communications on the roof and in the side mirror, where there is a small change in radiation patterns [3]. In MIMO sensitive characteristics like as the effects of the aperture (slit), coupling gap, and stub are investigated for improved impedance matching and bandwidth enhancement. MIMO antenna with grounded stubs and metamaterial are employed in to improve isolation and to achieve wide band phenomenon [4] [5].Ultra-wideband (UWB) MIMO technology is a promising approach for improving the efficiency of wireless communication systems. By using multiple antennas at both the transmitting and receiving ends, MIMO technology can increment the data rate, improve the precision of range estimates, reduce the power spectral density, and increase the wireless communication system's channel capacity [6]. UWB technology operates in a frequency band that is much wider than traditional wireless communication systems, which enables it to transmit more data in a given amount of time. The use of multiple antennas at both the receiver and transmitter can also improve the signal-to-noise ratio and reduce the amount of interference that a signal experiences. Overall, UWB MIMO technology has the potential to significantly enhance the performance and capacity of future wireless communication systems, making it a promising area of research and development processes and low-loss dielectric materials. Frequently microstrip antennas, slot antennas, and patch antennas are the printed antennas used for UWB MIMO systems. These antennas have advantages such as light weight, easy integration and low profile, with other electronic components [7]. Low gain, narrow bandwidth, and poor radiation efficiency are some of the antenna performance challenges caused while designing small size antennas. Metamaterials, adding slots and notches, and optimizing the geometries are just a few of the suggested ways to overcome these restrictions and enhance the performance of printed antennas for UWB MIMO systems. In

Ramamohan B and Siva Ganga Prasad M are with Dept. of ECE, Koneru Lakshmaiah Education Foundation, AP, India (email: ramamohanmailid@gmail.com, msivagangaprasad@kluniversity.in).

addition, the mutual coupling between the MIMO antennas can also have a significant impact on the overall performance of the system. To reduce the mutual coupling, various techniques have been proposed, such as using decoupling structures, spacing the antenna elements apart, and using polarization diversity. Overall, the integration of UWB and MIMO technologies in wireless communication systems has the potential to revolutionize the way that use and experience wireless communication. With the ongoing research and development in this field, we can expect even more advanced and efficient wireless communication systems in the near future. To reduce the mutual coupling within the radiating elements various methodologies' were proposed including use of Parasitic Elements (PE), which are additional structures that are located closely to the main antennas, but are not directly connected to the feed network [8] [9].These PEs can effectively decrease the interference between nearby antennas i.e. mutual coupling which is produced by generating a secondary radiation which is interfering with the main signal. Electromagnetic Band Gap (EBG) structures are specially designed materials that can manipulate electromagnetic waves and reduce their interaction between closely spaced elements [10] [11]. EBG structures have the ability to significantly reduce the interference caused by the mutual coupling between multiple MIMO antenna elements by providing a physical barrier between them. Decoupling and matching networks are used to minimize the mutual coupling by adjusting the impedance of the elements of antenna. These networks are designed to compensate for the impedance mismatches between the MIMO antenna elements, which can reduce the mutual coupling between them. Finally, neutralizing lines are another technique used to reduce mutual coupling in MIMO antennas. Neutralizing lines are additional conductive pathways that are located closely to the MIMO antenna elements. These lines has the ability to significantly reduce the interference caused by the mutual coupling between multiple MIMO antenna elements by generating a secondary current that interferes with the main signal. Overall, reducing mutual coupling in MIMO antennas is crucial for achieving high isolation and maintaining the system's performance. By combining different techniques and optimizing the design of the MIMO antenna, engineers and researchers can achieve the desired level of isolation and performance in small and portable size UWB MIMO antennas. In order to determine the optimal outcome for a given activity, a technique or process called optimization is used [12]. This optimization technique was invented in 1939 and was first known as linear programming [13] with quick and efficient execution, and it addresses the given issue. Many optimizing methods have been developed, including continuous optimization, global optimization, and derivative-free methods [14]. Antennas use the optimization process to improve their performance by fine-tuning various antenna characteristics using certain optimization methods [15]. The algorithms that underwent random search and sampling in order to complete an objective goal included bracketing, local descent, and stochastic algorithms. Not all domains call for a non-objective job that forbids any calculation of derivates. The term "black-box optimization" is used specifically to describe this kind of non-derivative calculation. Improving the performance and cost-effectiveness of complex, compact, and smart devices is the main focus of antenna optimization. Selecting suitable design parameters, variables, and constraints is critical for accomplishing these aims. Most antenna optimization problems have many objectives that, for optimal results, must be satisfied simultaneously. Because these objectives are mutually exclusive, it will be very difficult to find a solution that satisfies all of them. Two crucial considerations for antenna optimization are the likelihood of several local minima in the objective function and the expense of evaluating them. Finding the global minimum directly can be a challenging and burdensome task. Finding the best strategy for the optimization problem leads to appropriate design solutions. For instance, although some optimization challenges had simple potential answers, those solutions were only discovered after extensive time and investigation. These circumstances result in an improvement of the usual outcomes. The improved outcomes, however, could not also represent the global minimum [16]. Furthermore, the optimal solution to the given problem cannot be guaranteed or achieved using deterministic approaches. Stochastics solvers are therefore a superior alternative. To identify the best solution for a particular problem, some stochastic methods, such as the ant algorithm [17], genetic algorithm [18] and particle swarm optimization (PSO) [19] have demonstrated their effectiveness and reliability, their slow convergence is widely acknowledged. Furthermore, these approaches require a larger number of variables for optimization, which can further slowdown the process. and the more significant the number of variables, the more computing power is required [20]–[27]. The antenna optimization problem is thus rather contradictory; although the quickly executable approaches only carry local guarantees at the same time, the robust optimization strategies are probably going to have very sluggish convergence. So, it is important to choose the optimizing algorithms or optimizers carefully to ensure that they are compatible with the task at hand. In this work, we have optimized a MIMO antenna's structural parameters using genetic optimizer. The objectives are to achieve a -20 dB isolation and a UWB from 3.1 to 10.6 GHz. Since there are multiple objectives, the optimized parameters should lead to a UWB system that exhibits both strong gain and at least -20 dB of isolation. In prior studies and current works on antenna optimization approaches, researchers have primarily concentrated on optimizing antennas' parameters to achieve a specific goal, such as a higher operating frequency, radiation efficiency, gain, or isolation. Unfortunately, the multi-objective optimization problems are only briefly mentioned in relatively few articles. In order to achieve a UWB from 3.1 to 10.6 GHz, a decent gain of 4 dB - 6 dB in the operational range along with enhanced isolation of -20 dB, this work optimizes the antenna design. The suggested model's resonating frequencies are determined by two ground plane variables (sw and sl). Operating bands and other functional features are significantly affected by slight adjustments in the aforementioned variables. To operate the proposed antenna in UWB with -20 dB isolation, all two parameters are chosen at random. This sophisticated task requires more time and computing power to do manually. Hence this design task was changed

to an optimization task. To achieve the desired objectives, an optimization technique based on random search is utilized using the two parameters as the optimizing variables.

II. ANTENNA DESIGN

A. SISO Antenna Design

Initially, a Single Input Single Output (SISO) antenna was designed on the FR-4 substrate. The SISO antenna was used to build the proposed MIMO antenna design. A Upstox logo inspires this SISO antenna design. The SISO antenna design is simulated using the "Ansys High-Frequency Structure Simulator (HFSS) version R2 2022". The antenna design was fabricated using FR-4, which is a flame retardant - 4 material with advantages such as having good dielectric properties, can withstand high-temperature fluctuations and can offer large bandwidth, with a dimension of 22 x 21 x 1.5 mm^3.

- Iteration-1:

The SISO model was implemented using a half circle with a radius of 9 mm. This structure was fed using a 12 mm microstrip feed line, and this structure was supported by an entire ground plane with dimensions of 22 x 21 mm2 as shown in Fig. 1a. When excited, this structure was operating at 8.73 GHz, but the antenna return loss is less than -10 dB. Hence further modifications are attained to this structure to resonate in a wide band.

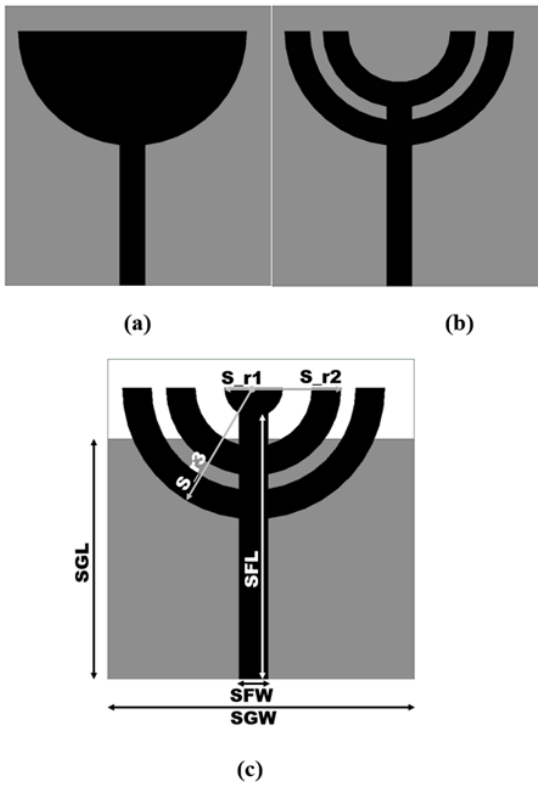

Fig. 1. Design steps of SEA: (a) step 1, (b) step 2, (c) step 3.

- Iteration-2:

To increase the antenna return loss and attain a wideband, a concentric half-circle structure was developed by extracting a 7 mm radius half-circle from the half-circle of a 9 mm radius. Further modifications are attained to develop another concentric half circle by removing a 4 mm radius half circle from the 6mm radius half circle, as shown below in Fig. 1b. These alterations were done to alter the surface currents in the patch. The ground in this iteration was a full ground structure with dimensions of 22 x 21 mm^2. This structure was operating at 7.73GHz with a return loss less than -10dB as illustrated in Fig. 2. Hence further modifications are attained to this structure to resonate in a wide band.

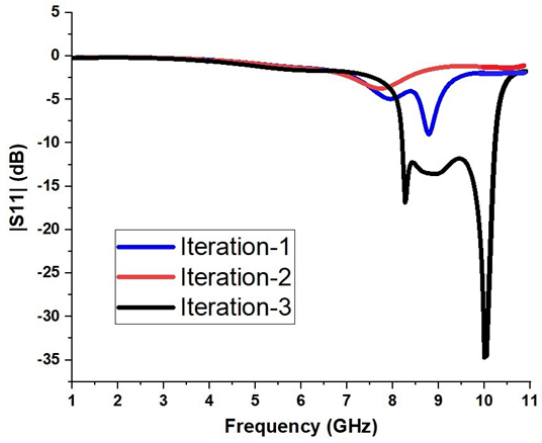

Fig. 2. Operating frequencies concerning SISO iterations.

- Iteration-3:

Another concentric half circle of a 2 mm radius is introduced into the half circle to increase the antenna bandwidth, as shown in Fig. 1c. The ground in this iteration was taken as more than half ground structure with dimensions of 16.5 x 21 mm2. The operating range frequency of this model is 4.8 GHz to 9.8 GHz, and it has a return loss of more than -20 dB. Hence a wideband frequency is obtained in this result. The overall parameters of the proposed antenna are given in Table 1. This proposed SISO antenna is used to implement the proposed MIMO antenna.

TABLE I
PROPOSED SISO ANTENNA PARAMETERS

S No	Term	Notation	Dimension(mm)
1	SISO Ground Length	SGL	16.5
2	SISO Ground Width	SGW	21
3	SISO Feed Length	SFL	9
4	SISO Feed Width	SFW	2
5	$Radius_1$	S_r1	2
6	$Radius_2$	S_r2	6
7	$Radius_3$	S_r3	9

B. MIMO Antenna Design

The proposed MIMO antenna was designed using three design steps, as seen in Fig. 3. By effective use of the design features of the developed SISO antenna, the dual-element

MIMO antenna is developed. The proposed MIMO antenna design was built on an FR-4 substrate with a dimension of 22 x 42 x 1.5 mm^3. The patch elements structure of the MIMO was constructed by mirroring the patch of the SEA design.

- Iteration-1:

Considering the results of the developed SISO antenna, the proposed MIMO model was implemented using two upside-down half circles with a radius of 9 mm each, as shown in Fig. 3a. These structures were fed using a micro-strip feed line of 12 mm, which was supported by an entire ground plane of 22 x 42 mm^2. When excited, this structure operated at 8.73 GHz, but the antenna return loss was less than -10dB as seen in Fig. 4. Hence further modifications are attained to this structure to resonate in a wideband.

- Iteration-2:

To increase the antenna return loss and attain a wideband, a concentric half circle of 7mm radius is detached from each half circle of 9mm radii, as shown in Fig. 3b. Further modifications are attained to develop another concentric half circle by removing the 4mm radii half circle from the 6mm radii half circle. The ground in this iteration was altered to a half-ground structure with dimensions of 11 x 42 mm^2. This structure obtained a good return loss value, i.e., -27.2dB. However, the antenna operates in dual bands at frequencies of 5.2 GHz and 6.7 GHz.

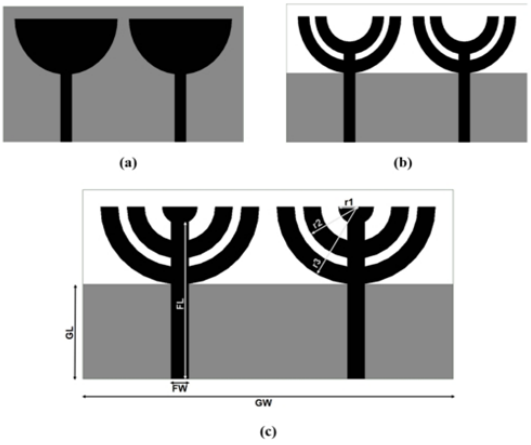

Fig. 3. Design steps of MIMO antenna: (a) step 1, (b) step 2, (c) step 3.

- Iteration-3:

To increase the antenna's bandwidth, another concentric half circle of 2 mm radius is introduced into both half circles, as shown in Fig. 3c. A similar half-ground was considered as like were being in the previous iteration. This specific model uses a broad spectrum that spans between 4.8 GHz to 9.8 GHz for operation. Hence a wide band was achieved as illustrated in Fig. 5. With these parameters a prototype was built and validated in the anechoic chamber, However, this model failed to achieve optimal parameters such as good isolation gain and efficiency. So, this particular model from iteration three was selected for further alterations.

The ground plane structure from the MIMO iteration three significantly impacts the antenna resonating characteristics.

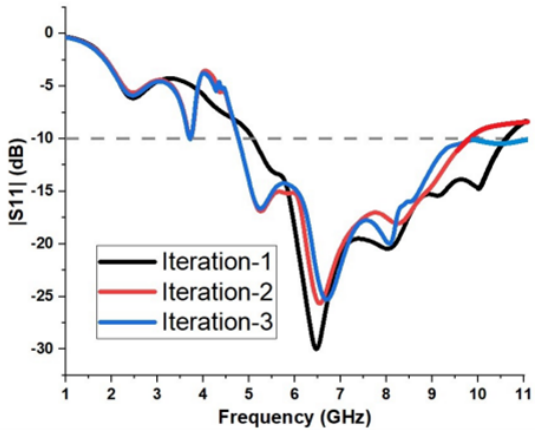

Fig. 4. Operating frequencies concerning MIMO design steps.

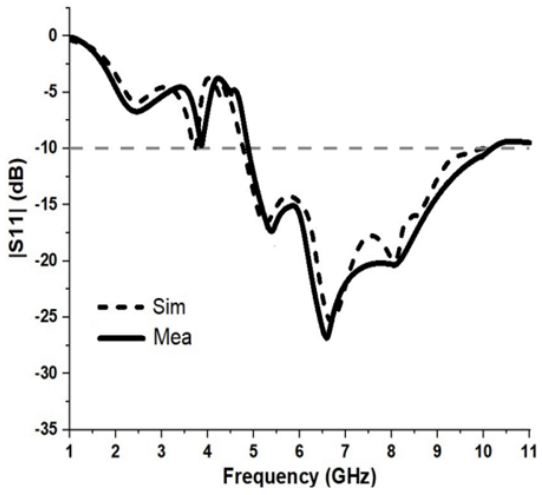

Fig. 5. Simulated and Measured Operating Frequencies before Optimization.

So, a primary focus was laid on its modification. A rectangular slot was opened on the ground plane structure with dimensions of 3 x 4 mm^2; with this modification, the antennas turned to operate at 4.6 GHz to 9.8 GHz. This rectangular slot showed a favourable result in achieving the required goals. So, the geometrical parameters of this slot sl and sw were parametrized to analyse the antennas resonating nature concerning the changes in the sl and sw. The results obtained from the parametric analysis failed to achieve the multi-objective goal. Observing these results concluded that a more advanced parametric analysis has to be performed on the two variables simultaneously. Hence MIMO antenna's structural parameters were optimized using a genetic optimizer. The objectives are to achieve a -20 dB isolation and a UWB from 3.1 to 10.6 GHz. Since there are multiple objectives, the optimized parameters should lead to a UWB system that exhibits both strong gain and at least -20 dB of isolation. In this work, a random search-based genetic optimizer was chosen, as optimizer because this algorithm explores a wider range of the search space, increasing the likelihood of finding

the global optimum solution and does not require a lot of prior knowledge about the problem being optimized.

TABLE II
PROPOSED SISO ANTENNA PARAMETERS

S No	Term	Notation	Dimension(mm)
1	Ground Length	GL	11
2	Ground Width	GW	42
3	Feed Length	FL	19
4	Feed Width	FW	2
5	Radius_1	r_1	2
6	Radius_2	r_2	6
7	Radius_3	r_3	9

III. OPTIMIZATION

Randomness is a fundamental aspect of the genetic algorithm (GA) and other evolutionary algorithms. In the GA, the search process is guided by generating new solutions through random changes to the current solutions, such as mutation and crossover. Mutation involves making small random changes to the genetic material of an individual, such as flipping a bit in a binary chromosome or adding a small value to a gene in a real-valued chromosome. Crossover involves combining genetic material from two parents to create new offspring, where the selection of the parents and the choice of crossover points are often made randomly. The use of randomness in the GA allows the search process to explore a wide range of potential solutions and avoid getting trapped in local optima. By generating new solutions through random changes to the current solutions, the GA can continue to search for better solutions over multiple generations.However, while randomness is an important aspect of the GA, it is also important to balance it with other factors such as selection pressure and elitism to ensure that the search process is efficient and effective. (ACO). the genetic algorithm (GA) is often referred to as a simple GA (SGA) due to its relatively straightforward implementation compared to other evolutionary algorithms (EAs) such as particle swarm optimization (PSO) or ant colony optimization [20]–[27].

In a genetic algorithm (GA), a population is a collection of candidate solutions, where each solution is represented as an individual. The population size, denoted as pop size, is the number of individuals in the population. Each individual has a chromosome that encodes its genetic information. The chromosome can be thought of as a string of symbols that represents the individual's genes, where each gene represents a particular parameter or feature of the individual. The specific form of the chromosome can vary depending on the problem being solved and the representation chosen by the GA designer. For example, in a binary GA, each gene might be a binary digit (0 or 1), while in a real-valued GA, each gene might be a real number. Other types of representations include permutation, tree-based, and graph-based representations. The goal of the GA is to evolve the population of individuals over time by using selection, crossover, and mutation operators to generate new individuals with different chromosomes that may be better suited to the problem at hand. The fitness of each individual is evaluated based on how well it solves the problem, and individuals with higher fitness are more likely to be selected for reproduction as shown in Fig. 6.

The fitness function is a mathematical function that evaluates the quality of a candidate solution represented by an individual in the population. The result of the fitness function is a fitness value that reflects how well the individual solves the problem being considered. In general, the higher the fitness value, the better the quality of the solution. The fitness function is problem-specific, and its design depends on the nature of the problem being solved. For example, in a maximization problem, the fitness function might return a fitness value that increases with the quality of the solution, while in a minimization problem, the fitness function might return a fitness value that decreases with the quality of the solution. The fitness values of the individuals in the population are used to guide the selection of individuals for reproduction in the GA. The individuals with higher fitness values are more likely to be selected for reproduction, and thus their genetic material is more likely to be passed on to future generations.

This selection process, along with the application of genetic operators such as crossover and mutation, can lead to the evolution of better solutions over time. By repeatedly generating new offspring and selecting the best individuals from each generation, the GA can gradually improve the quality of the solutions over time. However, it's important to balance the exploration of new solutions with the exploitation of promising solutions that have already been discovered, in order to achieve the best results. The selection process helps to improve the overall quality of the population by removing the low-quality individuals and promoting the high-quality ones. Over time, this can lead to the convergence of the population towards an optimal or acceptable solution, as the good properties are retained and the bad ones are discarded. Additionally, the use of crossover and mutation operations helps to introduce new genetic information into the population, which can further improve the quality of the solutions.

IV. RESULT AND DISCUSSIONS

A. Cost Function

The functional performance of the genetic optimizer can be analysed through the cost evaluation plot, depicted in Fig. 9. During each iteration, the genetic algorithm randomly selects a variable value from a pre-defined range. This selection process is arbitrary, as mentioned earlier. Using these selected values, the optimizer executes the simulation and validates the results with the predefined targets. If the targets are met, then chosen values for the variables are considered as the optimized values, and the cost value is set to zero. However, if the optimization condition or objectives are not met, new variable values are generated and the executed until the optimizer gets the cost value nearer or equal to zero. The GA optimizer was executed 226 times and produces the optimize value. With these results, using these optimal values the MIMO antenna was fabricated on a glass epoxy material and validated in an anechoic chamber.

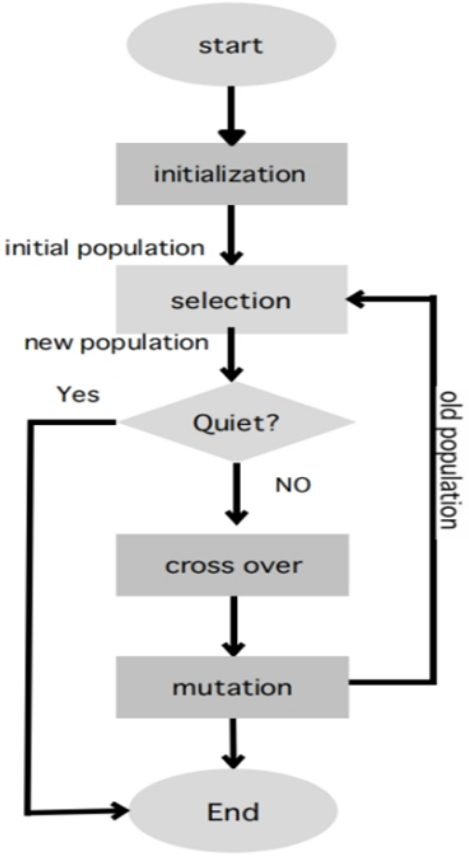

Fig. 6. Genetical Optimizer Working Mechanism

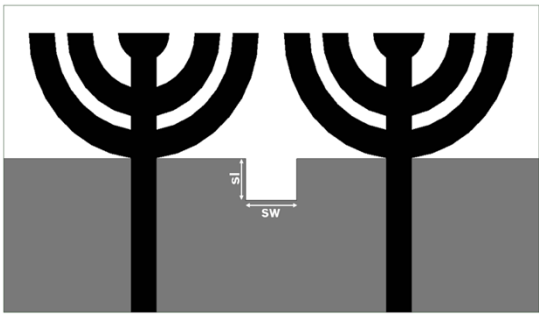

Fig. 7. Proposed MIMO model after Optimization.

Fig. 8. Fabricated Prototype.

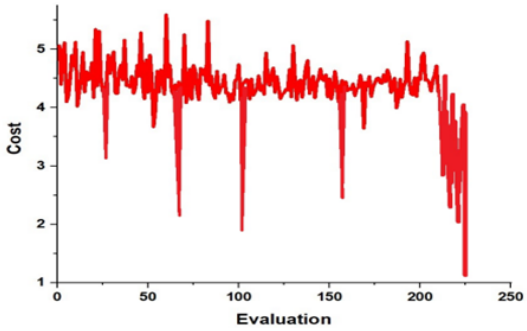

Fig. 9. Cost v/s Evaluation Plot

B. Final Simulated And Measured S-Parameters

The reflection coefficient S11 denotes the ratio between the reflected wave and the incident wave at the antenna's input port. It is an important parameter that characterizes the antenna performance. Evaluating the scattering parameters of a proposed antenna is an important step in the design process to ensure that the antenna meets the desired performance specifications. The Vector Network Analyzer (VNA) evaluates the two-port proposed prototype antenna's scattering parameters. The simulated and measured S11 values can be compared to assess the accuracy of the antenna design. The measured values closely match the simulated values as shown in Fig. 10, indicating that the prototype performs as expected.The measured and simulated mutual couplings among all ports of the proposed prototype antenna are given in Fig. 11. According to the illustration, it can be demonstrated that, throughout the whole operating UWB band, the mutual coupling is less than -20dB between the two elements. This indicates that there is high isolation between close parts of the antenna. High isolation between antenna elements is important because it helps to prevent interference between the elements, which can degrade the performance of the antenna. The fact that the mutual coupling is less than -20dB between any two components over the operating band is a desirable result and indicates that the proposed antenna design is effective in achieving good isolation.

C. Surface Current Density

Figure 12 represents the current density coupling analysis among the ports. The figure illustrates that when the first antenna element is activated by port 1, it exhibits surface density without any effect on the other antenna elements or with minimal effect, indicating little coupling. Similarly, activating the different antenna elements produces a little coupling effect on the remaining elements. The lack of significant coupling between the antenna elements is important because it indicates that each element can be excited independently without affecting the performance of the other elements. This can be advantageous in certain applications where multiple antennas are required to operate simultaneously but with minimal interference.

TABLE III
A COMPARATIVE STUDY AMONG THE PROPOSED ANTENNA WITH SOME RECENT LITERATURE.

S. No.	Material	Dimensions	Feed	Mutual Coupling	Optimization Algorithm	Frequency (in GHz)
[28]	Rogers	61 x 65 mm^2	Microstrip	< -15 dB	No	1.49 - 2.8, 4.9 - 5.10
[29]	FR-4	60 x 60 mm^2	Coaxial	-20 dB	No	1.99 - 2.8, 5.20 - 5.8
[30]	FR-4	77 x 52 mm^2	Microstrip	< -15 dB	No	2.4 - 2.5, 5.10 - 5.9
[31]	FR-4	80 x 48 mm^2	Coaxial	-20 dB	No	2.39 - 2.48, 5.14 - 5.95
[32]	FR-4	74 x 47.3 mm^2	Coaxial	-30 dB	No	2.47 - 2.8, 5.05 - 5.51
This Work	FR-4	22 x 42 mm^2	Microstrip	-20 dB	GA	UWB (3.1-10.6)

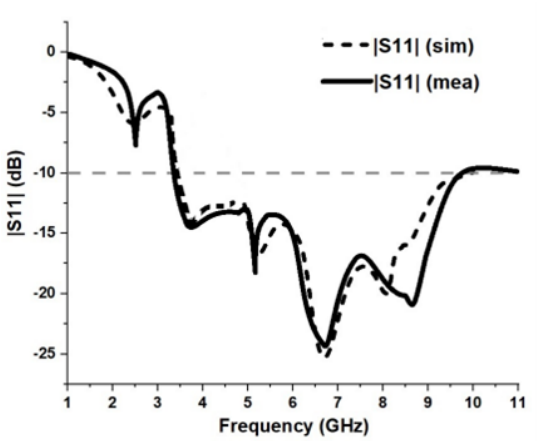

Fig. 10. Optimized Antenna Simulated and Measured S11/ S22.

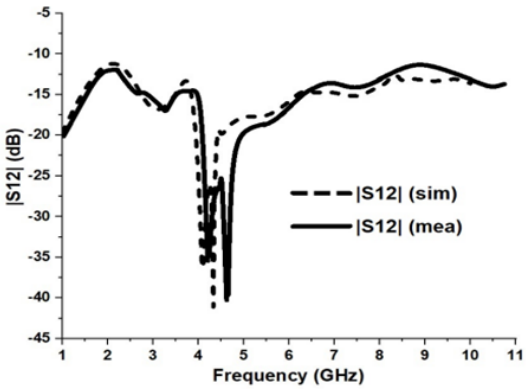

Fig. 11. Optimized Antenna Simulated and Measured S12/ S21.

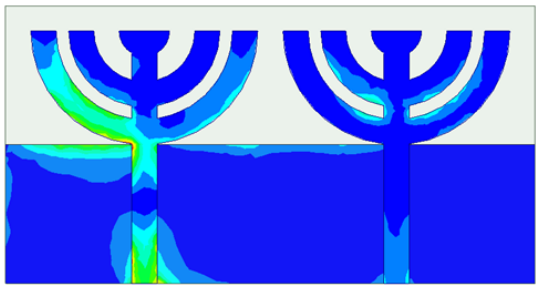

Fig. 12. Surface current distribution plot demonstrating low mutual coupling.

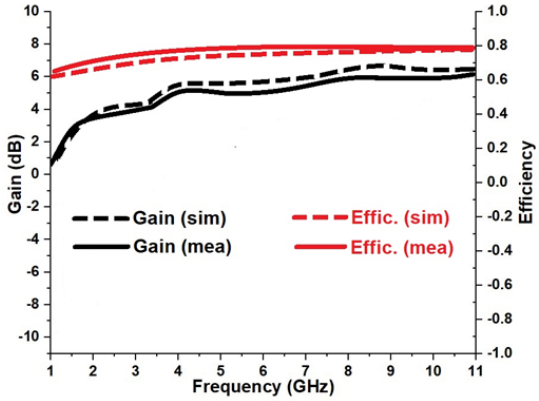

Fig. 13. Proposed antenna's simulated and measured Efficiency and Gain plot.

D. Gain and efficiency

In Figure 13, the simulated plot displays the efficiency and gain of the antenna. The results indicate a strong gain in frequencies in between 3.1 GHz - 10.6 GHz, with an efficiency of approximately 80% in the corresponding bands. These values suggest that the proposed MIMO has an operational ultra wideband capability with good efficiency. Overall, the successful optimization of the given task by the optimizer is supported by these values, which have been verified through measurements of the prototype. A comparative study among the proposed antenna with some literature is provided in Table 3.

V. CONCLUSION

A designed wideband MIMO was made into an ultra-wideband antenna using an optimization technique. A genetic

optimization-based multiple-objective approach is employed in this case to optimize the design using random search-based optimization. For the optimization, the ground structure was modified by introducing a rectangular slot with a length (sl) and width (sw) were used as variables. The optimal values from the preset ranges have been effectively discovered by the random search-based method. The cost function graph is used to determine the ideal value, and this technique achieves the least expensive value of 0.23412. These values are used to construct the antenna on FR-4 and validate it in an anechoic environment. In both the simulation and the measurement, a good acceptability range was identified. The dual requirements of achieving ultra-wideband (UWB) and improving isolation to -20 dB throughout the whole Ultra Wideband and S11 becoming under -10 dB between 3.1 to 10.6 GHz have been successfully met by the multi-objective optimization. The gain and radiation patterns were scrutinized the entire UWB, and their accuracy was confirmed through measurements conducted in an anechoic chamber. These confirmed results demonstrate the outstanding efficacy of the genetic optimizer in transforming a multi-band antenna into a UWB antenna.

ACKNOWLEDGMENT

The authors of this paper affirm that they are free from any relationships or financial conflicts of interest that may have impacted their work.

REFERENCES

[1] S. Modak, T. Khan, T. A. Denidni, and Y. M. M. Antar, "Miniaturized self-isolated uwb mimo planar/cuboidal antenna with dual x-band interference rejection," *AEU-Int. J. Electron. Commun.*, vol. 143, p. 154020, Jan 2022. [Online]. Available: https://doi.org/10.1016/j.aeue.2021.154020

[2] A. S. A. El-Hameed, M. G. Wahab, N. A. Elshafey, and M. S. Elpeltagy, "Quad-port uwb mimo antenna based on lpf with vast rejection band," *AEU-Int. J. Electron. Commun.*, vol. 134, p. 153712, May 2021. [Online]. Available: https://doi.org/10.1016/j.aeue.2021.153712

[3] S. Arumugam, S. Manoharan, S. K. Palaniswamy, and S. Kumar, "Design and performance analysis of a compact quad-element uwb mimo antenna for automotive communications," *Electronics*, vol. 10, no. 18, p. 2184, Sep 2021. [Online]. Available: https://doi.org/10.3390/electronics10182184

[4] B. Yeboah-Akowuah, E. T. Tchao, M. Ur-Rehman, M. M. Khan, and S. Ahmad, "Study of a printed split-ring monopole for dual-spectrum communications," *Heliyon*, vol. 7, no. 9, p. e07928, Sep 2021. [Online]. Available: https://doi.org/10.2139/ssrn.3886316

[5] M. H. Reddy, D. Sheela, V. K. Parbot, and A. Sharma, "A compact metamaterial inspired uwb-mimo fractal antenna with reduced mutual coupling," *Microsyst. Technol.*, vol. 27, no. 5, pp. 1971–1983, May 2021. [Online]. Available: https://doi.org/10.1007/s00542-020-05024-z

[6] S. Ahmad, U. Ijaz, S. Naseer, A. Ghaffar, M. A. Qasim, F. Abrar, N. O. Parchin, C. H. See, and R. Abd-Alhameed, "A jug-shaped cpw-fed ultra-wideband printed monopole antenna for wireless communications networks," *Appl. Sci.*, vol. 12, no. 2, p. 821, Jan 2022. [Online]. Available: https://doi.org/10.3390/app12020821

[7] T. Addepalli and V. R. Anitha, "A very compact and closely spaced circular shaped uwb mimo antenna with improved isolation," *AEU-Int. J. Electron. Commun.*, vol. 114, p. 153016, Feb 2020. [Online]. Available: https://doi.org/10.1016/j.aeue.2019.153016

[8] M. S. Khan, S. A. Naqvi, A. Iftikhar, S. M. Asif, A. Fida, and R. M. Shubair, "A wlan band-notched compact four element uwb mimo antenna," *Int. J. RF Microw. Comput.-Aided Eng.*, vol. 30, no. 9, p. e22282, Sep 2020. [Online]. Available: https://doi.org/10.1002/mmce.22282

[9] D. A. Sehrai, F. Muhammad, S. H. Kiani, Z. H. Abbas, M. Tufail, and S. Kim, "Gain-enhanced metamaterial based antenna for 5g communication standards," *Comput., Mater. Continua*, vol. 64, no. 3, pp. 1587–1599, 2020. [Online]. Available: https://doi.org/10.32604/cmc.2020.011057

[10] N. A. Jan, S. H. Kiani, F. Muhammad, A. Sehrai, A. Iqbal, M. Tufail, and S. Kim, "V-shaped monopole antenna with chichen itza inspired defected ground structure for uwb applications," *CMC Comput. Mater. Continua*, vol. 65, pp. 19–32, Jul 2020. [Online]. Available: https://doi.org/10.32604/cmc.2020.011091

[11] Z. Li, C. Yin, and X. Zhu, "Compact uwb mimo vivaldi antenna with dual band-notched characteristics," *IEEE Access*, vol. 7, pp. 38 696–38 701, 2019. [Online]. Available: https://doi.org/10.1109/ACCESS.2019.2906338

[12] S. Etoz, C. L. Brace, N. A. Jan, S. H. Kiani, F. Muhammad, A. Sehrai, A. Iqbal, M. Tufail, and S. Kim, "V-shaped monopole antenna with chichen itza inspired defected ground structure for uwb applications," *CMC Comput. Mater.*, 2024.

[13] M. R. Kılınç and N. V. Sahinidis, "Exploiting integrality in the global optimisation of mixed-integer nonlinear programming problems with baron," *Optim. Methods Softw.*, vol. 33, pp. 540–562, Apr 2018. [Online]. Available: https://doi.org/10.1080/10556788.2017.1350178

[14] S. Arora and S. Singh, "Butterfly optimisation algorithm: a novel approach for global optimisation," *Soft Comput.*, vol. 23, pp. 715–734, Feb 2019.

[15] W. Deng, J. Xu, and H. Zhao, "An improved ant colony optimisation algorithm based on hybrid strategies for scheduling problem," *IEEE Access*, vol. 7, pp. 20 281–20 292, Feb. 2019. [Online]. Available: https://doi.org/10.1109/ACCESS.2019.2897580

[16] S. Koziel and A. Pietrenko-Dabrowska, "Expedited feature-based quasi-global optimisation of multi-band antenna input characteristics with jacobian variability tracking," *IEEE Access*, vol. 8, pp. 83 907–83 915, May 2020. [Online]. Available: https://doi.org/10.1109/ACCESS.2020.2992134

[17] R. K. Verma and D. K. Srivastava, "Optimisation and parametric analysis of slotted microstrip antenna using particle swarm optimisation and curve fitting," *International Journal of Circuit Theory and Applications*, vol. 49, pp. 1868–1883, Jul. 2021. [Online]. Available: https://doi.org/10.1002/cta.2957

[18] R. G. Mishra, R. Mishra, P. Kuchhal, and N. P. Kumari, "Optimisation and analysis of high gain wideband microstrip patch antenna using genetic algorithm," *International Journal of Engineering and Technology*, vol. 7, pp. 176–179, May 2018. [Online]. Available: https://doi.org/10.14419/ijet.v7i1.5.9142

[19] Y.-H. Fang, W.-S. Zhao, F.-K. Lin, D.-W. Wang, J. Wang, and W.-J. Wu, "An amc-based liquid sensor optimised by particle-ant colony optimization algorithms," *IEEE Sensors Journal*, vol. 22, pp. 2083–2090, Feb. 2021. [Online]. Available: https://doi.org/10.1109/JSEN.2021.3133688

[20] M. S. Khan, A. Capobianco, M. F. Shafique, B. Ijaz, A. Naqvi, and B. D. Braaten, "Isolation enhancement of a wideband mimo antenna using floating parasitic elements," *Microwave and Optical Technology Letters*, vol. 57, no. 7, pp. 1677–1682, 2015. [Online]. Available: https://doi.org/10.1002/mop.29162

[21] I. Adam, M. N. M. Yasin, N. Ramli, M. Jusoh, H. A. Rahim, T. B. A. Latef, T. F. T. M. N. Izam, and T. Sabapathy, "Mutual coupling reduction of a wideband circularly polarized microstrip MIMO antenna," *IEEE Access*, vol. 7, pp. 97 838–97 845, 2019. [Online]. Available: https://doi.org/10.1109/ACCESS.2019.2928899

[22] M. Farahani, J. Pourahmadazar, M. Akbari, M. Nedil, A. R. Sebak, and T. A. Denidni, "Mutual coupling reduction in millimeter-wave MIMO antenna array using a metamaterial polarization-rotator wall," *IEEE Antennas and Wireless Propagation Letters*, vol. 16, pp. 2324–2327, 2017. [Online]. Available: https://doi.org/10.1109/LAWP.2017.2717404

[23] Y. Li, L. an Bian, Y. Liu, Y. Wang, R. Chen, and S. Xie, "Mutual coupling reduction for monopole MIMO antenna using l-shaped stubs, defective ground and chip resistors," *AEU-International Journal of Electronics and Communications*, p. 154524, 2023. [Online]. Available: https://doi.org/10.1016/j.aeue.2022.154524

[24] V. Dhasarathan, T. K. Tran, J. Kulkarni, B. Garner, and Y. Li, "Mutual coupling reduction in dual-band MIMO antenna using parasitic dollar-shaped structure for modern wireless communication," *IEEE Access*, 2023. [Online]. Available: https://doi.org/10.1109/ACCESS.2023.3235761

[25] F. Urimubenshi, D. B. Konditi, J. de Dieu Iyakaremye, P. M. Mpele, and A. Munyaneza, "A novel approach for low mutual coupling and ultra-compact two port MIMO antenna development for UWB

wireless application," *Heliyon*, vol. 8, no. 3, p. e09057, 2022. [Online]. Available: https://doi.org/10.1016/j.heliyon.2022.e09057

[26] A. Ali, J. Tong, J. Iqbal, U. Illahi, A. Rauf, S. U. Rehman, H. Ali, M. M. Qadir, M. A. Khan, and R. M. Ghoniem, "Mutual coupling reduction through defected ground structure in circularly polarized, dielectric resonator-based MIMO antennas for sub-6 GHz 5G applications," *Micromachines*, vol. 13, no. 7, p. 1082, 2022. [Online]. Available: https://doi.org/10.3390/mi13071082

[27] M. Elahi, A. Altaf, E. Almajali, and J. Yousaf, "Mutual coupling reduction in closely spaced MIMO dielectric resonator antenna in H-Plane using closed metallic loop," *IEEE Access*, vol. 10, pp. 71 576–71 583, 2022. [Online]. Available: https://doi.org/10.1109/ACCESS.2022.3187433

[28] Q. Li, M. Abdullah, and X. Chen, "Defected ground structure loaded with meandered lines for decoupling of dual-band antenna," *Journal of Electromagnetic Waves and Applications*, vol. 33, pp. 1764–1775, Jun. 2019. [Online]. Available: https://doi.org/10.1080/09205071.2019.1643261

[29] P. Liu, D. Sun, P. Wang, and P. Gao, "Design of a dual-band MIMO antenna with high isolation for WLAN applications," *Progress In Electromagnetics Research Letters*, vol. 74, pp. 23–30, Apr. 2018. [Online]. Available: https://doi.org/10.3390/electronics10141659

[30] D. Shen, L. Zhang, Y. Jiao, and Y. Yan, "Dual-element antenna with high isolation operating at the WLAN bands," *Microwave and Optical Technology Letters*, vol. 61, pp. 2323–2328, Oct. 2019. [Online]. Available: https://doi.org/110.1002/mop.31901

[31] J. Deng, J. Li, L. Zhao, and L. Guo, "A dual-band inverted-f MIMO antenna with enhanced isolation for WLAN applications," *IEEE Antennas and Wireless Propagation Letters*, vol. 16, pp. 2270–2273, Jun. 2017. [Online]. Available: https://doi.org/10.1109/LAWP.2017.2713986

[32] J. Y. Deng, Z. J. Wang, J. Y. Li, and L. X. Guo, "A dual-band MIMO antenna decoupled by a meandering line resonator for WLAN applications," *Microwave and Optical Technology Letters*, vol. 60, pp. 759–765, Mar. 2018. [Online]. Available: https://doi.org/10.1002/mop.31049